Free Radical Biology & Medicine, Vol. 28, No. 11, pp. 1589–1597, 2000

0891-5849/00/$–see front matter

PII S0891-5849(00)00275-6

Original Contribution

TWO-PHOTON MICROSCOPY OF AORTA FIBERS SHOWS PROTEOLYSIS INDUCED BY LDL HYDROPEROXIDES

TIZIANA PARASASSI,*† WEIMING YU,† DIANE DURBIN,‡ LIANA KURIASHKINA,§ ENRICO GRATTON,† NOBUYO MAEDA,‖ and FULVIO URSINI¶

*Istituto di Medicina Sperimentale, CNR, Roma, Italy; †Laboratory for Fluorescence Dynamics, Department of Physics, University of Illinois at Urbana-Champaign, Urbana, IL, USA; ‡Department of Biochemistry, University of Illinois College of Medicine at Urbana-Champaign, Urbana, IL, USA; §Department of Molecular and Integrative Physiology, University of Illinois at Urbana-Champaign, Urbana, IL, USA; ‖Department of Pathology, School of Medicine, University of North Carolina, Chapel Hill, NC, USA; and ¶Dipartimento di Chimica Biologica, Universita' di Padova, Padova, Italy

(*Received* 29 *February* 2000; *Revised* 23 *March* 2000; *Accepted* 30 *March* 2000)

Abstract—Oxidatively modified LDL mimics several aspects of atherogenesis. In this disease, degradation of the matrix proteins' network also occurs. By a new morphological ex vivo approach, not requiring sample processing, we explored the relationship between the degradation of matrix protein and oxidatively modified LDL. Two-photon excitation fluorescence microscopy images of fresh cross-section rings of rat aorta, acquired while the sample was maintained in a glucose- and oxygen-supplemented buffer, showed straight, parallel, thick, long extracellular matrix proteins. Traditional microscopic examination, requiring sample fixation and staining, shows smaller and curved fibers. Instead, we observed curved and broken fibers after a 30-min incubation of aorta with either LDL containing lipid hydroperoxides, or *tert*-butyl-hydroperoxide. The adhesion of LDL to the endothelium and its internalization was directly visualized by using a lipid fluorophore. The damage to aorta matrix proteins induced by LDL and *tert*-butyl-hydroperoxide was fully prevented by antioxidants, such as ascorbate or Trolox C, or inhibitors of proteases. The image spectroscopy of the fibers' autofluorescence (polarization and lifetime) revealed an increased mobility of the fluorescent cross-link in fibers. Damaged matrix proteins were also imaged in aorta samples from apolipoprotein E knock-out mice. Our ex vivo images directly visualized the activation of a fast redox-sensitive proteolytic process in the arterial wall triggered by lipid hydroperoxides in LDL. © 2000 Elsevier Science Inc.

Keywords—Autofluorescence, LAURDAN, Matrix protein, Oxidation, Two-photon microscopy, Free radicals

INTRODUCTION

Age-dependent degeneration of the arterial wall involves increased wall thickness, decreased elasticity, disorganization and fragmentation of elastic fibers, and usually develops together with the formation of lipid plaque, the typical hallmark of atherogenesis [1–3]. Aneurysm formation and evolution involves degradation of matrix proteins [4]. Endothelial dysfunction, eventually evolving to vascular damage, can be reproduced in vitro by low-density lipoprotein (LDL), oxidatively modified to various extents [5–9]. Endothelial dysfunctions encompass the alteration of the endothelial barrier and the expression of adhesion molecules recruiting macrophages, which transmigrate to the subendothelial space together with LDL. Focus has been directed to the presence of lipid hydroperoxides or oxysterols in LDL [8,9], on LDL particle size [6], on a covalent linkage to apo(a) [5], and on the role of inflammation in promoting gene activation [7]. Recent reports highlight the participation of LDL in the proteolysis of vascular extracellular matrix by inducing (i) a decrease of macrophage-specific tissue inhibitors of matrix-degrading metalloproteinases through the modulation of interleukin-8 [10]; (ii) the upregulation of expression of metalloproteinase-9 in monocytes, together with the downregulation of the metalloproteinase-1 inhibitor [11]; and (iii) the upregulation of the expression of the membrane type 1 matrix metalloproteinase in endothelial cells [12].

Enzymes with elastolytic activity [2,13] have a phys-

Address correspondence to: Tiziana Parasassi, Istituto di Medicina Sperimentale, CNR, Viale Marx 15-43, 00137 Roma, Italy; Tel: +39 (06) 86090.316; Fax: +39 (06) 86090.332; E-Mail: tiziana@biocell.irmkant.rm.cnr.it.

iological role in the growth and turnover of elastic fibers in the vascular system, lungs, and skin, and are modulated by specific inhibitors [14,15]. In the lungs, oxidation of the active site of elastase inhibitor primes the degradation of the extracellular matrix [14]. Elastase activity has been suggested to be involved in the pathogenesis of abdominal aortic aneurysm [4,16] as well as in remodeling of the vasculature occurring in aging [2].

In this study, we directly visualized the effect of minimally-oxidized LDL on the degradation of extracellular proteins in fresh rat aorta by means of two-photon near-infrared excitation microscopy [17–19]. This microscopy does not require sample treatment such as freezing-thawing, inclusion in matrices, fixation or staining [20–22], which may produce artifacts, e.g., contraction produced by fixation, which dehydrates the sample. By its deeper penetration in highly scattering tissues vs. light of shorter wavelengths, the near-infrared excitation allows imaging of interior regions of intact tissues, with a penetration of about 200 μm [23]. Typical features of two-photon excitation microscopy include the simultaneous absorption of two near-infrared photons with a total energy equivalent to one photon, at half of the wavelength. Therefore, absorption in the ultraviolet region can be achieved by near-infrared excitation with the advantage of strongly reducing the sample photodamage and photobleaching, usually associated with UV excitation. In the absence of exogenous fluorophores, a variety of autofluorescence signals can be observed [18,23], arising from molecules absorbing in the UV range (one-photon absorption). We obtained for the first time high-resolution images of the intense autofluorescence arising from extracellular matrix proteins of a fresh rat aorta. The matrix proteins' fluorescence emission was also characterized by measuring polarization and lifetime, pixel by pixel, as a function of the LDL-induced damage.

We report clear evidence that lipid hydroperoxides in LDL activate a redox-sensitive proteolytic system that degrades vascular matrix proteins. The vascular damage produced by oxidatively modified LDL is quite similar to the damage visualized in the aorta of apo-E knock-out mice [24], a well-known model of vascular damage and atherosclerosis.

MATERIALS AND METHODS

Preparation of aorta samples and incubation with LDL

Aorta cross-section rings, about 0.5 mm thick, were sectioned from the ascending aorta of 6- to 8-week-old Long-Evans male rats, and from ascending or descending aorta of apoE $-/-$ [24] or $+/+$ mice using a tissue chopper, immediately after the animals were sacrificed. Samples were maintained in Earle's balanced salt solution (EBSS) containing 24.6 mmol/l glucose, 26.3 mmol/l $NaHCO_3$, pH 7.4, saturated with 95% O_2 and 5% CO_2. Samples were imaged within a few hours by mounting in a hanging drop slide in fresh EBSS buffer. Human LDL at a protein concentration of 3 mg/ml, or 50 μmol/l *tert*-butyl-hydroperoxide (TBH), were added to aorta rings and incubated for 30 min at 37°C. In some experiments, the incubation medium also contained one of the following: 0.1 mmol/l ascorbic acid, 0.1 mmol/l Trolox C, 2.3 g/l α-1-antitrypsinase, or 3 g/l of eglin-c. Unless specified, materials were from Sigma Chemical Co. (St Louis, MO, USA). The animals used in this study were maintained, and the tissue was prepared, in agreement with institutional and federal guidelines for the humane treatment of animals.

Preparation of LDL, of minimally oxidized LDL and measurement of their lipid hydroperoxide content

Human LDL was prepared from healthy fasting volunteers by routine ultracentrifugation [25]. Lipid hydroperoxides in LDL were increased by storage of dialyzed LDL at 4°C for 7–15 d. The storage for up to 2–3 months produces the so called "minimally oxidized LDL" [26]. We used a rather short storage period, during which only lipid hydroperoxides are reported to increase [26], virtually without other apparent oxidative damage, i.e., production of aldehydes, consumption of vitamin E, modification of apo-B charge.

Lipid hydroperoxide concentration in human LDL and in mouse plasma was measured using the kinetic test based on the best-fitting of the decay of chemiluminescence emission of luminol in the presence of hemin, as previously described [27].

Labeling of vascular cells and of LDL

A lipophilic probe, 2-dimethylamino-6-lauroyl-naphthalene (LAURDAN) (Molecular Probes Inc., Eugene OR, USA) was used to visualize cells in the space between matrix fibers. Three μl of a 2 mmol/l solution of LAURDAN in dimethylsulfoxide were added to 3 ml of EBSS, containing the aorta ring and minimally oxidized LDL, and incubated for 30 min at 37°C. Labeled samples were then washed and mounted in fresh EBSS medium for microscopic observations.

Microscopy measurements

The 770 nm beam was from a titanium-sapphire laser (Mira 900, Coherent, Palo Alto, CA, USA) pumped by an argon ion laser (Innova 310, Coherent). The microscope configuration and scanning routine

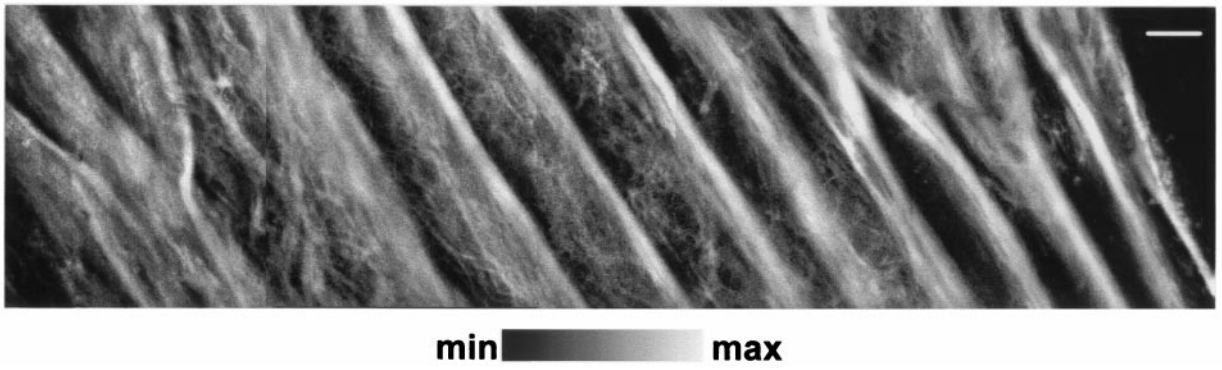

Fig. 1. Composite image of several adjacent frames of deep optical sections showing the autofluorescence intensity of the matrix fibers in a control sample of a rat aorta cross-section ring from the lumen (right) to the ring exterior (left). The bar corresponds to 10 μm.

was previously described [19]. A frame scanning rate of 20 s was used. The average laser power on the sample was on the order of 3 mW. A quarter-wave plate was used to change the laser light polarization from linear to circular. Autofluorescence was collected through a broad band BG39 barrier filter. Because we did not use UV optics, tryptophan and tyrosine fluorescence did not interfere with the fibers' autofluorescence. For polarization measurements, a vertically polarized two-photon excitation was obtained by inserting a polarizer after the quarter-wave plate in the excitation path. The autofluorescence emission was collected after an analyzer, inserted into the optical path. Images of parallel and perpendicular emission were used to calculate the images of autofluorescence polarization. The polarization was not corrected for the instrument geometry. Images of LAURDAN-labeled samples were acquired using two different optical bandpass filters (Ealing Electro Optics, New Englander Industrial Park, Holliston, MA, USA) centered in the blue (440 nm) and in the red (490 nm) regions of the LAURDAN emission spectrum. The two filters were exchanged each time a full frame was scanned. From the images at the two emissions, the generalized polarization (GP) [28] image was calculated as previously described [29]. The lifetime images were obtained using the microscope configuration described in [19] and using the harmonic response technique. The Ti-Sapphire laser was operated with a repetition rate of 80 MHz and a pulse width of 150 fs. The autofluorescence emission was detected by a gain-modulated photomultiplier. The laser source, detection system, and computer comprise a phase-locked loop. The images of the demodulation and of the phase shift were used to calculate the modulation lifetimes and the phase lifetimes images using an image of a fluorescein solution in water as the reference, as described in [19].

RESULTS

A representative image of two-photon excitation autofluorescence of deep optical section of rat aorta cross-section rings, acquired while the tissue was maintained in a glucose- and oxygen-supplemented buffer, is reported in Fig. 1. An intense autofluorescence arising from fibers was observed. Thick fibers show a regular, parallel organization and are interconnected by a complex network of smaller fibrils.

Elastin and collagen in matrix fibers show similar emission spectra [30], originating from desmosine and pyridinoline cross-links, respectively [22]. The fluorescence polarization value obtained from aorta autofluorescence images and from purified elastin images were quite similar (0.38 ± 0.01 and 0.40 ± 1, respectively), supporting the morphological identification.

In our images, the NAD(P)H autofluorescence [23] was very low in comparison to that arising from fibers, and not resolvable from the background.

To image the vascular tissue, including cells between matrix fibers, we used an environment-sensitive lipophilic fluorescent probe (LAURDAN), which labels cell membranes and lipids in LDL. LAURDAN emission was analyzed by calculating the GP value [28,29] at each pixel, thus producing a pseudo-color GP image. Figure 2A is a pseudo-color representative image of the LAURDAN GP, in the aorta cross-section ring, where red (high GP) endothelial cells are facing the lumen and yellow-green (low GP) smooth muscle cells are visible in the space between the matrix fibers. In this figure, extracellular matrix proteins are seen in blue due to the typical low GP value of their autofluorescence in our experimental conditions.

LAURDAN-labeled LDL was visible in the aorta tissue after incubation with 3 mg/ml of minimally oxidized human LDL, containing 15–30 nmoles of lipid hydroperoxides/mg of cholesterol, for 30 min at 37°C.

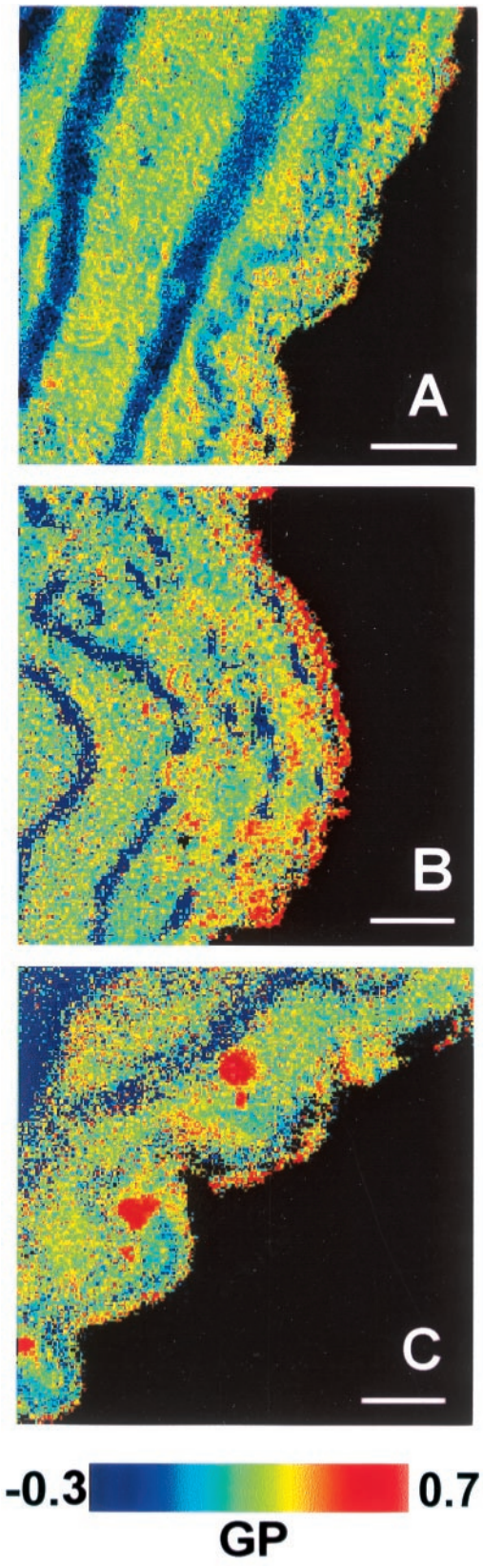

Fig. 2. Pseudo-color representation of LAURDAN GP values (range from −0.3 = blue to 0.7 = purple) in rat aorta sections. In panel A, a control samples is imaged; in panels B and C the aorta samples were incubated for 30 min at 37°C with minimally oxidized LDL. In all panels, the lumen is on the right. The bar corresponds to 10 μm.

Our spectroscopic measurements of LAURDAN-labeled minimally oxidized LDL gave relatively high GP values, of about 0.46 ± 0.01. In Figs. 2B and 2C, LDL particles are redder than the endothelial cell membranes. In Fig. 2B, LDL is adhering to the endothelium, while in Fig. 2C it is compartmentalized in the subendothelial space as aggregates. Adhering and compartmentalized LDL was simultaneously present in different areas of all aorta samples after incubation with LDL. Extracellular fibers appeared curved and with some fragmentation. The modification of the morphology of extracellular matrix proteins after a 30 min incubation with minimally oxidized LDL was also observed by a direct autofluorescence imaging, without the LAURDAN labeling, and similar to the image reported in Fig. 1. Curves, invaginations, and ruptures were produced (Figs. 3A–D), the alterations being most relevant in fibers facing the lumen. Control samples, incubated for 30 min at 37°C in the absence of LDL, did not show any changes in the structure of the fibers. Similar alterations, although to a more limited extent, were observed in aorta fibers after incubation with freshly prepared LDL, still containing about 1–4 nmoles of lipid hydroperoxides/mg of cholesterol (not shown).

The addition of antioxidants such as ascorbate or Trolox C, a water soluble analog of Vitamin E, to the incubation medium fully prevented the degradation of the matrix network induced by minimally oxidized LDL (Figs. 3E–F).

The involvement of proteolytic enzymes was investigated by adding protease inhibitors such as α-1-antitrypsinase [14] or the specific inhibitor of elastase eglin-c [31]. Both inhibitors fully prevented alteration of fibers induced by minimally oxidized LDL (Figs. 3G–H).

Incubation with *tert*-butyl-hydroperoxide (TBH) also produced curved, curly and broken fibers (Fig. 4), thus supporting a specific role of lipid hydroperoxides in LDL. Antioxidants and protease inhibitors prevented the damage induced by TBH (not shown).

To better characterize the spectroscopic features of the fiber autofluorescence associated with degradation, the polarization and the fluorescence lifetimes were measured at every pixel of the autofluorescence images. After incubation with minimally oxidized LDL, the polarization of matrix protein autofluorescence decreased from 0.38 ± 0.01 to 0.29 ± 0.01 (average values of three images) (Fig. 5). As shown in Fig. 6, the decrease of the polarization value is related to the incubation time with LDL. In Fig. 6, the autofluores-

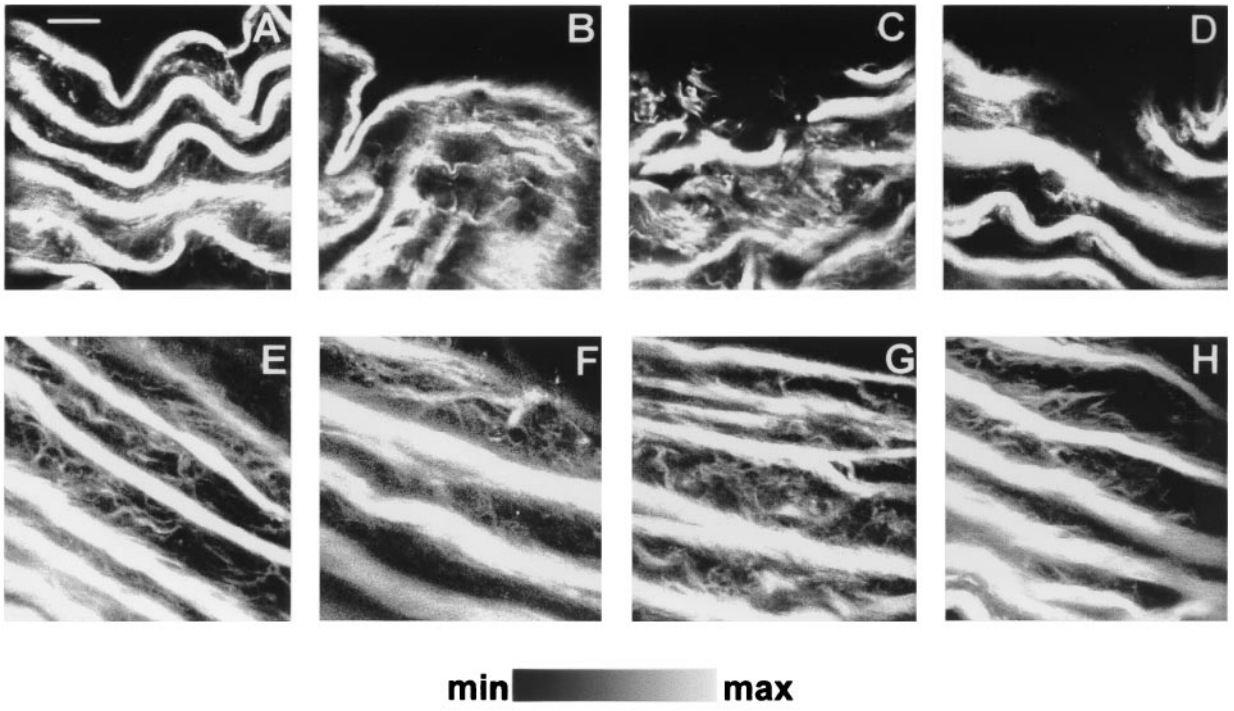

Fig. 3. Representative images of autofluorescence intensity of the extracellular matrix proteins in deep optical sections of rat aorta rings, following treatment with (A–D) minimally oxidized LDL in the presence of (E) 0.1 mmol/l ascorbic acid, (F) 0.1 mmol/l Trolox C, (G) 2.3 g/l α-1-antitrypsinase, and (H) 3 g/l eglin-c. In all panels, the lumen is on the top. The bar corresponds to 10 μm.

cence polarization value of the aorta fibers after incubation with TBH is also reported. Both in controls and in treated samples, the autofluorescence lifetimes of fibers was relatively low, centered at about 2 ns, and continuously distributed in a range between 0.01 and 6 ns. Due to this complex decay, the average lifetime change after treatment was rather small, with an average 6% decrease in the center of the lifetime distribution (average of three images).

The occurrence in vivo of a similar degradation of aorta matrix network was verified in apolipoprotein E-deficient mice (apoE $-/-$) [24], a well known and suitable model of atherosclerosis. Aorta rings of apoE $-/-$ mice cut at the location of atheromatous plaques showed extremely curly and thin fibers (Fig. 7A), while rings from areas apparently free of plaque showed thicker fibers, although still curved (Fig. 7B). These last images were quite similar to those of aorta rings of control mice after incubation with minimally oxidized LDL (Fig. 7C). Instead, fibers of control

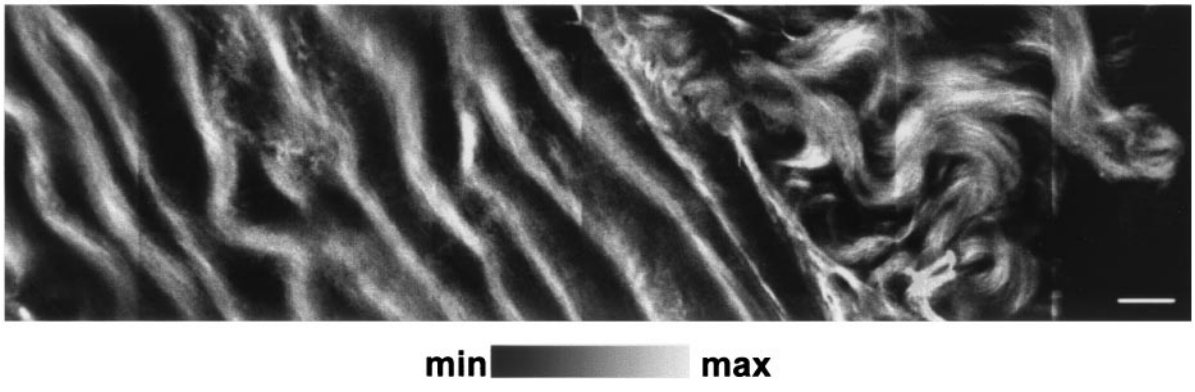

Fig. 4. Representative example of the morphology of aorta matrix fibers after incubation with *tert*-butyl-hydroperoxide (TBH), 50 mM for 30 min at 37°C. Composite image of several adjacent frames of deep optical sections showing the autofluorescence intensity of the matrix fibers in the aorta cross-section ring from the lumen (right) to the ring exterior (left). The bar corresponds to 10 μm.

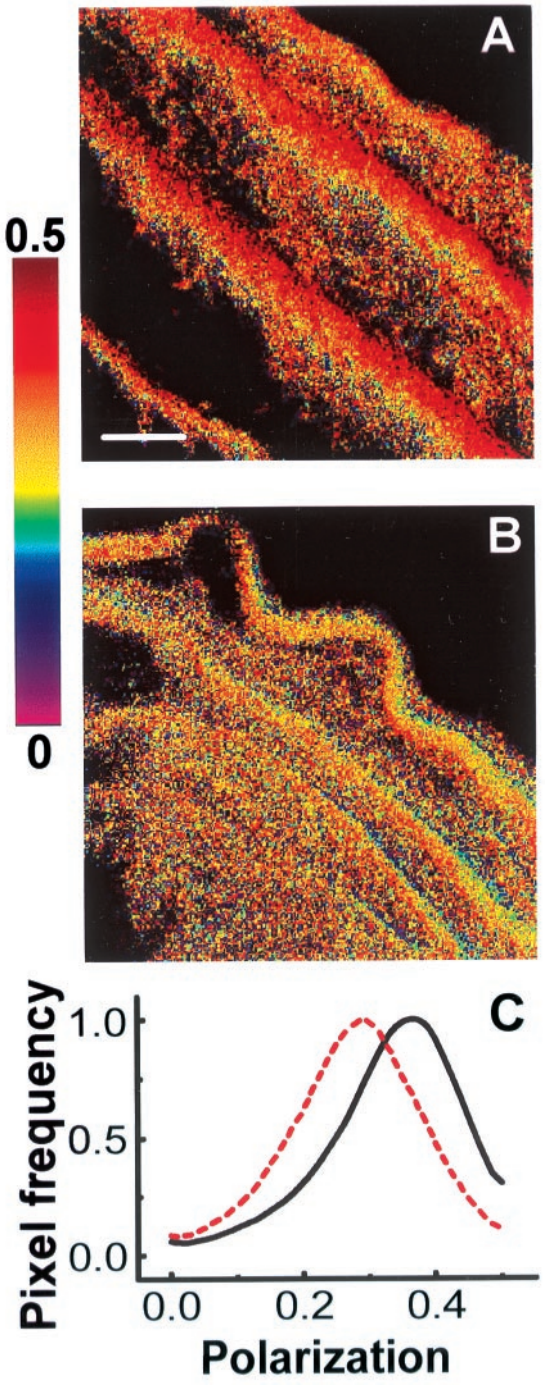

Fig. 5. Examples of pseudo-color representation of autofluorescence polarization values (ranging from 0 = violet to 0.5 = red) of matrix fibers in (A) control aorta ring and (B) after incubation with minimally oxidized LDL. Lumen is on top right. The bar corresponds to 10 μm. (C) Normalized histograms of the pixel frequency vs. autofluorescence polarization values were obtained from the corresponding images for the control (continuous black line) and for the ox-LDL-treated sample (dotted red line). Each histogram represents the average of three images.

(+/+) mice showed the usual straight and thick fibers (not shown), similar to those of control rats. In

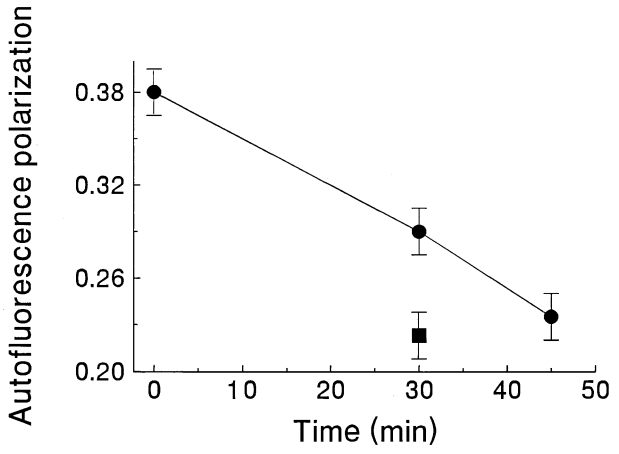

Fig. 6. Polarization values of the autofluorescence of aorta extracellular matrix proteins as a function of the incubation time with minimally oxidized LDL (●) and with 50 μM TBH for 30 min (■). The points represent the maximum pixel frequency of the polarization histograms (obtained as in the legend of Fig. 5) averaged over 3 to 5 different polarization images.

apoE −/− mice, in addition to hypercholesterolemia (1.6 ± 0.6 mg/ml vs. 0.4 ± 0.1 mg/ml in the control mice), we measured an even more significant increase in the concentration of plasma lipid hydroperoxides (0.6 ± 0.3 μmol/l vs. 0.1 ± 0.04 μmol/l in the control).

DISCUSSION

Two features characterize the most common degenerative process of arterial wall, the focal formation of plaque with the related thrombotic outcome, and a diffuse loss of elastic properties due to thickening of the wall and to degradation of matrix fibers, also known as the vasculopathy of aging [1–3]. Degradation of matrix proteins, particularly elastin, is also involved in plaque rupture and aneurysm [4,16]. We now present evidence for the activation of proteolysis in the vascular matrix network specifically induced by lipid hydroperoxides in LDL.

In our short-term incubation of fresh aorta rings, we used LDL with a limited amount of lipid hydroperoxides, ≤ 30 nmol/mg of cholesterol, a concentration 10–20 times lower than in copper-oxidized LDL, usually referred to as ox-LDL [32], and in the "minimally oxidized LDL" obtained by storage for 2–4 months [26]. Notably, the level of lipid hydroperoxides in our minimally oxidized LDL is below the detection limit of usual analytical tests, so that unless a chemiluminescence method is used, they would be considered as native "nonoxidized" LDL. Moreover, also in freshly prepared LDL we detected hydroperoxides, although at a level never exceed-

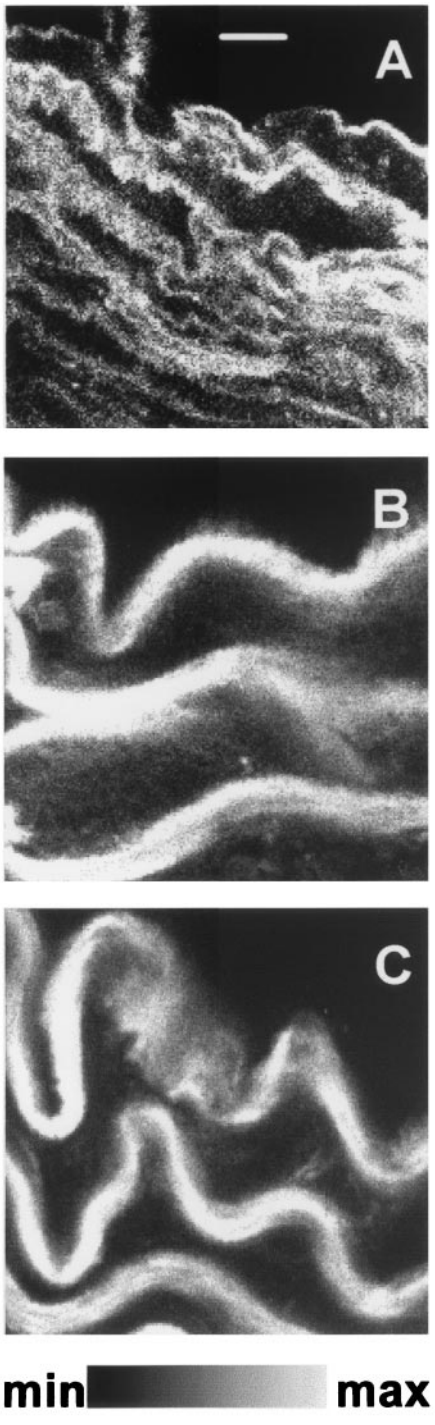

Fig. 7. Representative images of autofluorescence intensity of the extracellular matrix proteins in deep optical sections of mouse aorta cross-section rings. Rings were sectioned from transgenic apoE −/− mice aorta (A) at the location of a plaque and (B) in areas apparently free of plaque. (C) The rings from control (+/+) mice have been treated with minimally oxidized LDL. In all panels, the lumen is on top. The bar corresponds to 5 μm.

ing 1–4 nmoles/mg cholesterol. In our experiments, even these fresh LDL damaged the vascular matrix network, although less massively than the minimally oxidized LDL.

By using the lipophilic fluorescent probe LAURDAN, adhesion of LDL particles to the endothelium and its internalization can be followed with no need of tissue fixation nor of specific antibodies. The LAURDAN probe diffuses into tissue lipids and, due to its virtually complete partitioning into lipids with respect to the aqueous environment, its labeling persists while the tissue is imaged in its buffer. The value of LAURDAN GP allows the identification of LDL particles in the GP image because the cholesterol-rich LDL displays a GP value higher than that of vascular cell membranes [33].

The direct visualization of proteolytic damage induced by minimally oxidized LDL has been made possible by the use of a technique that minimizes the sample treatment. We used rat aorta slices, sectioned by a tissue chopper immediately after the animals were sacrificed, maintained and observed in a glucose- and oxygen-supplemented buffer. In contrast, images obtained by conventional microscopy are obtained from slices thinner by at least one order of magnitude and following freezing-thawing, inclusion in matrices, fixation, and staining, with the result that thin and curly fibers are also imaged in control samples [20–22]. Our images show a regular organization of long, parallel, straight, and thick fibers, which is lost only after exposure to oxidants in LDL.

Contraction of smooth muscle cells in the vasculature could also modify the shape of extracellular matrix proteins, producing curved fibers. LDL has been reported to inhibit the ability of blood vessels to relax [34], to induce a further contraction in vessels pretreated with contractile agonists [35], and to make vessels more prone to vasospasm in response to contractile stimuli [36]. However, no contraction-inducing agonists were used in this study, and no apparent contraction was observed upon addition of LDL. Further, following treatment of the aorta with minimally oxidized LDL, we did observe a massive fiber fragmentation, which cannot be accounted for by an artifactual contraction.

The decreased autofluorescence polarization and the slightly shorter lifetime measured after treatment with minimally oxidized LDL or TBH fits the morphological fragmentation, indicating an increased mobility and a more hydrophilic environment of the fluorescent cross-link in fibers. The polarization value seems particularly appropriate for the quantitative evaluation of the fibers' proteolysis.

While the protection exerted by antioxidants probed the oxidative nature of the primary event leading to proteolysis, the actual role of lipid hydroperoxides is supported by the following evidences: (i) TBH reproduces the effect; (ii) fresh LDL, containing a very low concentration of hydroperoxides, induces least damage;

and (iii) lipid hydroperoxides are the unique oxidation product detectable in LDL after short autoxidation, in the absence of catalyst transition metals.

The evidence presented indicates the involvement of an oxidation-sensitive mechanism leading to an enhanced activity of proteases on the extracellular matrix proteins. The underlying mechanism must relate to two not necessarily self-excluding options: (i) vascular cells challenged with the oxidative stimulus release proteases, or (ii) the oxidation directly inhibits an antiprotease. Our short incubation time and the analogy with the proteolytic damage occurring in lungs when challenged with oxidants favor of the second mechanism. In lungs, specific oxidation of the active site in the α-1-antiprotease leads to proteolysis of elastic fibers in the extracellular matrix [14]. Due to the short-term incubation required to observe the fibers' damage in our experiments, we do not expect an activation of gene expression to be involved [9,11,12]. The ox-LDL-induced activation of expression of metalloproteinases has been reported to peak in 6 h [12], after exposure to a concentration of LDL hydroperoxides much higher than that in the LDL we used.

The experiments on apoE $-/-$ mice, where the plasma concentration of lipid hydroperoxide is six times above control values, confirm the in vivo occurrence of fiber degradation. In plaques, the arterial matrix network is almost fully destroyed, and plaque-free areas display alteration similar to that observed in our ex vivo model. An appealing suggestion from these data is that oxidatively modified LDL leads to diffuse damage of vascular matrix, similar to the vasculopathy of aging, but plaque formation occurs only in discrete focal areas, in agreement with the suggestion that other elements, e.g., shear stress, are likely to be involved in plaque formation [37]. The more severe degradation of the fibrillar network observed under the plaque (Fig. 7A) supports a progression in the matrix damage.

In conclusion, our results demonstrate the involvement of a redox-sensitive proteolytic mechanism involved in the damage to vascular matrix proteins that is mediated by lipid hydroperoxides in LDL. In vivo, such an event can be due to the imbalance between the activation of proteases or inhibition of antiproteases, and an inadequate defense system including low levels of antiproteases and antioxidants. Finally, our data highlight a role of an optimized diet that minimizes oxidation of plasma lipids and increases antioxidant defense [38], thus affecting not only the development of the plaque, but also preventing the loss of elastic properties of the vasculature.

Acknowledgements — This work was supported by NIH RR03155 (T.P., W.Y., E.G.), in part by the Italian National Research Council (T.P.), and by the Italian Ministry of University and Scientific Research (F.U.).

REFERENCES

[1] Ross, R. The pathogenesis of atherosclerosis: a perspective for the 1990s. *Nature* **362:**801–808; 1993.
[2] Robert, L.; Robert, A. M.; Jacotot, B. Elastin-elastase-atherosclerosis revisited. *Atherosclerosis* **140:**281–295; 1998.
[3] Steinberg, D. Low density lipoprotein oxidation and its pathobiological significance. *J. Biol. Chem.* **272:**20963–20966; 1997.
[4] Thompson, R. W.; Baxter, B. T. MMP inhibition in abdominal aortic aneurysm. Rationale for a prospective randomized clinical trial. *Ann. NY Acad. Sci.* **878:**159–178; 1999.
[5] Nielsen, L. B. Atherogenicity of lipoprotein(a) and oxidized low density lipoprotein: insight for in vivo studies of arterial wall influx, degradation and efflux. *Atherosclerosis* **143:**229–243; 1999.
[6] Griffin, B. A. Lipoprotein atherogenicity: an overview of current mechanisms. *Proc. Nutr. Soc.* **58:**163–169; 1999.
[7] Yla-Herttuala, S. Oxidized LDL and atherogenesis. *Ann. NY Acad. Sci.* **874:**134–137; 1999.
[8] Patel, R. P.; Darley-Usmar, V. M. Molecular mechanisms of the copper dependent oxidation of low-density lipoproteins. *Free Radic. Res.* **30:**1–9; 1999.
[9] Brown, A. J.; Jessup, W. Oxysterols and atherosclerosis. *Atherosclerosis* **142:**1–28; 1999.
[10] Moreau, M.; Brocheriou, I.; Petit, L.; Ninio, E.; Chapman, M. J.; Rouis, M. Interleukin-8 mediates downregulation of tissue specific inhibitor of metalloproteinase-1 expression in cholesterol-loaded human macrophages: relevance to stability of atherosclerotic plaques. *Circulation* **99:**420–426; 1999.
[11] Xu, X. P.; Meisel, S. R.; Ong, J. M.; Kaul, S.; Cercek, B.; Rajavashisth, T. B.; Sharifi, B.; Shah, P. K. Oxidized low-density lipoprotein regulates matrix metalloproteinase-9 and its tissue inhibitor in human monocyte-derived macrophages. *Circulation* **99:**993–998; 1999.
[12] Rajavashisth, T. B.; Liao, J. K.; Galis, Z. S.; Tripathi, S.; Laufs, U.; Tripathi, J.; Chai, N. N.; Xu, X. P.; Jovinge, S.; Shah, P. K.; Libby, P. Inflammatory cytokines and oxidized low density lipoproteins increase endothelial cell expression of membrane type 1-matrix metalloproteinase. *J. Biol. Chem.* **274:**11924–11929; 1999.
[13] George, S. J. Tissue inhibitors of metalloproteinases and metalloproteinases in atherosclerosis. *Curr. Opin. Lipidol.* **9:**413–423; 1998.
[14] Evans, M. D.; Pryor, W. A. Cigarette smoking, emphysema, and damage to alpha 1-proteinase inhibitor. *Am. J. Physiol.* **266:** L593–L611; 1994.
[15] Tyagi, S. C.; Kumar, S. G.; Alla, S. R.; Reddy, H. K.; Voelkler, D. J.; Janicki, J. S. Extracellular matrix regulation of metalloproteinase and antiprotease in human heart fibroblast cells. *J. Cell. Physiol.* **167:**137–147; 1996.
[16] Curci, J. A.; Liao, S.; Huffman, M. D.; Shapiro, S. D.; Thopson R. W. Expression and localization of macrophage elastase (Matrix metalloproteinase-12) in abdominal aortic aneurysm. *J. Clin. Invest.* **102:**1900–1910; 1998.
[17] Denk, W.; Strickler, J. H.; Webb, W. W. Two-photon laser scanning fluorescence microscopy. *Science* **248:**73–76; 1990.
[18] Bennett, B. D.; Jetton, T. L.; Ying, G.; Magnuson, M. A.; Piston, D. W. Quantitative subcellular imaging of glucose metabolism within intact pancreatic islets. *J. Biol. Chem.* **271:**3647–3651; 1996.
[19] Konig, K.; So, P. T.; Mantulin, W. W.; Tromberg, B. J.; Gratton, E. Two-photon excited lifetime imaging of autofluorescence in cells during UVA and NIR photostress. *J. Microsc.* **183:**197–204; 1996.
[20] de Carvalho, H. F.; Taboga, S. R. Fluorescence and confocal laser scanning microscopy imaging of elastic fibers in hematoxylin-eosin stained sections. *Histochem. Cell. Biol.* **106:**587–592; 1996.
[21] Young, A. A.; Legrice, I. J.; Young, M. A.; Smaill, B. H. Extended confocal microscopy of myocardial laminae and collagen network. *J. Microsc.* **192:**139–150; 1998.
[22] Baraga, J. J.; Rava, R. P.; Fitzmaurice, M.; Tong, L. L.; Taroni, P.; Kittrell, C.; Feld, M. S. Characterization of the fluorescent

morphological structures in human arterial wall using ultraviolet-excited microspectrofluorimetry. *Atherosclerosis* **88:**1–14; 1991.
[23] Masters, B. R.; So, P. T.; Gratton, E. Multiphoton excitation fluorescence microscopy and spectroscopy of in vivo human skin. *Biophys. J.* **72:**2405–2412; 1997.
[24] Bronson, S. K.; Plaehn, E. G.; Kluckman, K. D.; Hagaman, J. R.; Maeda, N.; Smithies, O. Single-copy transgenic mice with chosen-site integration. *Proc. Natl. Acad. Sci. USA* **93:**9067–9072; 1996.
[25] Havel, R. J.; Howard, A. E.; Bragdon, J. H. The distribution and chemical composition of ultracentrifugally separated lipoproteins in human serum. *J. Clin. Invest.* **34:**1345–1349; 1955.
[26] Berliner, J. A.; Territo, M. C.; Sevanian, A.; Ramin, S.; Kim, J. A.; Bamshad, B.; Esterson, M.; Fogelman A. M. Minimally modified low density lipoprotein stimulates monocyte endothelial interactions. *J. Clin. Invest.* **85:**1260–1266; 1990.
[27] Pastorino, M. A.; Zamburlini, A.; Zennaro, L.; Maiorino, M.; Ursini, F. Measurement of lipid hydroperoxides in human plasma and lipoproteins by kinetic analysis of photon emission. *Methods Enzymol.* **300:**33–39; 1998.
[28] Parasassi, T.; De Stasio, G.; d'Ubaldo, A.; Gratton, E. Phase fluctuation in phospholipid membranes revealed by Laurdan fluorescence. *Biophys. J.* **57:**1179–1186; 1990.
[29] Yu, W. M.; So, P. T.; French, T.; Gratton, E. Fluorescence generalized polarization of cell membranes: a two-photon scanning microscopy approach. *Biophys. J.* **70:**626–636; 1996.
[30] Baraga, J. J.; Rava, R. P.; Taroni, P.; Kittrel, C.; Fitzmaurice, M.; Feld, M. S. Laser induced fluorescence spectroscopy of normal and atherosclerotic human aorta using 306–310 nm excitation. *Laser Surg. Med.* **10:**245–261; 1990.
[31] Faller, B.; Dirrig, S.; Rabaud, M.; Bieth, J. G. Kinetics of the inhibition of human pancreatic elastase by recombinant eglin c. Influence of elastin. *Biochem. J.* **270:**639–644; 1990.
[32] Weidtmann, A.; Scheithe, R.; Hroboticky, N.; Lorenz, R.; Siess, W. Mildly oxidized LDL induces platelet aggregation through activation of phospholipase A2. *Arterioscler. Thromb. Vasc. Biol.* **15:**1131–1138; 1995.
[33] Parasassi, T.; Di Stefano, M.; Loiero, M.; Ravagnan, G.; Gratton, E. Influence of cholesterol on phospholipid bilayers phase domains as detected by Laurdan fluorescence. *Biophys. J.* **66:**120–132; 1994.
[34] Matthys, K. E.; Van Hove, C. E.; Kockx, M. M.; Andries, L. J.; Van Osselaer, N.; Herman, A. G.; Bult, H. Exposure to oxidized low-density lipoproteins in vivo enhances intimal thickening and selectively impairs endothelium-dependent dilation in the rabbit. *Cardiovasc. Res.* **37:**239–246; 1998.
[35] Simon, B. C.; Cunningham, L. D.; Cohen, R. A. Oxidized low density lipoproteins cause contraction and inhibit endothelium-dependent relaxation in the pig coronary artery. *J. Clin. Invest.* **86:**75–79; 1990.
[36] Galle, J.; Bassenge, E.; Busse, R. Oxidized low density lipoproteins potentiate vasoconstrictions to various agonists by direct interaction with vascular smooth muscle. *Circ. Res.* **66:**1287–1293; 1990.
[37] Fatouraee, N.; Deng, X.; De Champlain, A.; Guidoin, R. Concentration polarization of low density lipoprotein (LDL) in the arterial system. *Ann. NY Acad. Sci.* **858:**137–146; 1998.
[38] Ursini, F.; Zamburlini, A.; Cazzolato, G.; Maiorino, M.; Bittolo-Bon, G.; Sevanian, A. Postprandial lipid hydroperoxides: a possible link between diet and atherosclerosis. *Free Radic. Biol. Med.* **25:**250–252; 1998.